JOURNAL OF MATERIALS SCIENCE 27 (1992) 1347–1352

Investigation of the decomposition behaviour in supersaturated Al–Zn alloys

A. GABER, N. AFIFY
Physics Department, Faculty of Science, Assiut University, Assiut, Egypt

The decomposition behaviour in supersaturated Al + (1–6.4) at % Zn has been investigated using electrical resistivity and microhardness measurements in the temperature range from room temperature to ~500° C. The experimental results showed that (i) both the temperature coefficient of resistivity and the relaxation time of the free electrons diminish as the concentration of Zn increases in the alloy; (ii) the early stage decomposition of the supersaturated alloys via Guinier–Preston zone formation is accompanied by an appreciable increase in the microhardness of about 80 MPa per 1 at % Zn; (iii) the obtained activation energy of 0.41 eV for the precipitation process of the dissolved zinc atoms is close to the migration energy of zinc in aluminium which indicates that the precipitation mechanism is characterized by the migration and coalescence of zinc atoms.

1. Introduction

In most aluminium alloys, the dissolved elements have a decreasing solubility with decreasing temperature. Therefore, when the alloy is given a solution heat treatment and then quenched to a temperature equal or near to room temperature, it will be supersaturated with respect to the dissolved element and will undergo structural changes. These structural transformations have been widely investigated in supersaturated binary and ternary aluminium alloys. In Al–Zn alloys, the early stage decomposition process is characterized by the formation of small spherical zones within the crystal lattice (Guinier–Preston, GP, zones), rich in solute atoms and coherent with the matrix. The GP zone formation was found to take place during ageing of the quenched alloys at or near room temperature. A progressive evolution of transition phases has been detected in Al–Zn alloys before the development of stable precipitates [1]. The X-ray diffraction technique has been used to determine the sequence of phase transitions that occur during the pre-precipitation stage in Al–Zn solid solutions. The following precipitation sequence has been concluded [1]: spherical GP zones → ellipsoidal GP zones → rhombohedral transition phase → α' cubic transition phase → zinc-rich stable precipitates.

Techniques of small-angle X-ray scattering (SAXS) [2–6], transmission electron microscopy (TEM) [5–7], positron annihilation (PA) [8], electrical resistivity [5, 9–11] and the microhardness tests [9, 10, 12–14] have been successfully used to follow the decomposition behaviour of the supersaturated aluminium binary and ternary alloys as a function of temperature.

Owing to the sensitivity of the electrical resistivity and the microhardness of the metallic solid solutions to their structural changes, following these quantities for the supersaturated Al–Zn alloys as a function of temperature may provide evidence of their internal structural changes. It has been reported that a simultaneous increase in microhardness and electrical resistivity occurs due to the early stage decomposition and GP zone formation [15, 16]. In the present work, the electrical resistivity and microhardness measurements were used to follow the decomposition behaviour of the solute atoms in Al–Zn alloys as a function of temperature.

2. Experimental procedure

In order to study the decomposition behaviour in Al–Zn alloys, specimens of aluminium with 1, 1.3, 3.2, 3.9, 5.2 and 6.4 at% Zn were prepared, which are referred to as AZ1, AZ1.3, AZ3.2, AZ3.9, AZ5.2 and AZ6.4, respectively. The specimens were prepared using pure aluminium (99.98%) and pure zinc (99.9%). The specimens were then homogenized for 10 h at 500 °C and spectroscopically analysed in the physical laboratory of Naga-Hammady Aluminium Society using an emission quantimeter type ARL 3400. The results of the analysis showed that the main impurities were iron and silicon of maximum content of 0.008 and 0.02 wt%, respectively. Disc-shaped specimens of 25 mm diameter and 2 mm thickness were machined from the prepared alloys.

Electrical resistivity measurements were carried out on the disc-shaped specimens using the Goretzki method. In this technique, the electrical resistivity could be measured on the disc-shaped specimens as accurately as on rods or wires. The details of the Goretzki method have been described elsewhere [10]. By this method, the measured resistivity could be reproduced to a precision better than 0.01 μΩ cm.

0022–2461

Microhardness measurements, HV, were made using the Vickers method. The basis of this method is indenting the well-polished surface of the disc-shaped specimens using a diamond square-based pyramid under a load of 0.49 N for a constant period of 10 s. The error in HV arises from the measurements of the diagonal impression which have an uncertainty of $\pm$ 0.168 μm. This leads to an error in HV not more than 1.2%.

3. Results

3.1. Dependence of the temperature coefficient of resistivity on the concentration of the dissolved zinc

An attempt is made below to present evidence for the effect of alloying on the temperature coefficient of resistivity. In the case of binary alloys in a solid solution state, the carrier mobility is attenuated by scattering on the lattice imperfections. If c is the atomic fraction of the dissolved zinc in aluminium, the carrier mobility, μ_{all}, can be described by the following approximate relation [17]

$$\mu_{all} = \beta'/[c(1 - c)] \quad (1)$$

where β' is a proportionality factor. Thus, the residual resistivity due to the solute zinc atoms can be given as

$$\rho_{res} = \beta c(1 - c) \quad (2)$$

where $\beta = 1/en\beta'$, where e is the electron's charge and n is the concentration of the free electrons per unit volume. This term for resistivity is independent of temperature and does not vanish at absolute zero. At temperatures other than absolute zero, a resistivity, $\rho(T)$ due to electron–phonon scattering is added to the residual resistivity (Matthiessen's rule). Therefore, the resistivity of the binary alloy at the given temperature, T, can be written

$$\rho_{all}^{(T)} = \beta c(1 - c) + \rho_T \quad (3)$$

For pure aluminium, $\rho_{all}^{(T)} = \rho_T$ and therefore, the temperature coefficient of resistivity, $\alpha = (1/\rho_T)(d\rho_T/dT)$. For binary alloys, the temperature coefficient of resistivity, α_{all}, should be

$$\alpha_{all} = (1/\rho_{all}^{(T)})(d\rho_{all}^{(T)}/dT) \quad (4)$$

Then

$$\alpha_{all} = \alpha/[1 + \beta c(1 - c)/\rho_T] \quad (5)$$

It follows from Equation 5 that α_{all} should be less than α of pure aluminium. Equation (5) can be rewritten

$$\alpha_{all}/\alpha = 1/[1 + \beta c(1 - c)/\rho_T] \quad (6)$$

According to Equation 3, the measured resistivity at room temperature (25 °C) of the specimens is represented against the product of the fractional constituents of the alloy, $c(1 - c)$ (Fig. 1). A value for β of 46.667 $\times 10^{-6}$ Ωcm can be determined. With the help of Equation 5, the values of α_{all} of the alloy for the given specimens were calculated and are listed in Table I. It can be observed that α_{all} diminishes with increasing zinc content, Fig. 2a. According to Equation 5, $1/\alpha_{all}$ varies linearly with $c(1 - c)$, Fig. 2b. Moreover, one

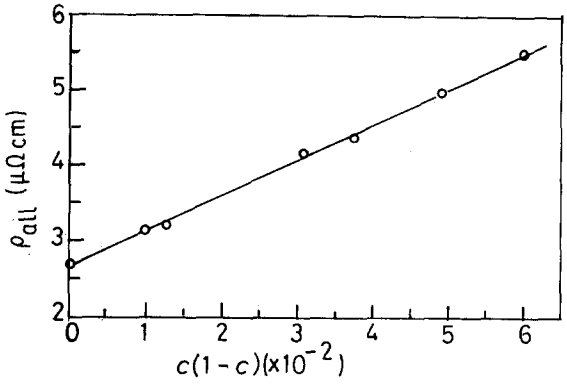

Figure 1 Variation of the electrical resistivity, ρ_{all} of the quenched specimens as a function of c $(1 - c)$.

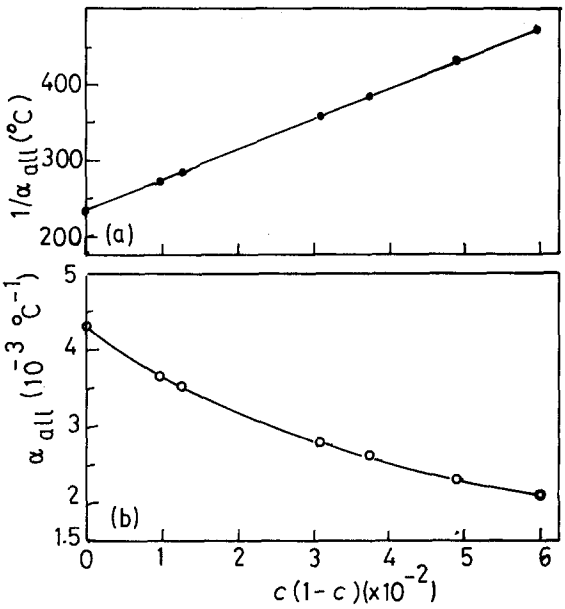

Figure 2 Effect of the concentration of the dissolved zinc on the temperature coefficient of resistivity, α_{all}, of Al–Zn alloys.

TABLE I

Specimen	Pure Al	AZ1	AZ1.3	AZ3.2	AZ3.9	AZ5.2	AZ6.4
$\alpha_{all}\,10^{-3}\,°C^{-1}$	4.29[a]	3.66	3.50	2.79	2.60	2.32	2.11
τ_{all}/τ	1.00	0.856	0.822	0.655	0.611	0.544	0.496

[a][19]

can easily deduce that the decrease of α_{all} with c reaches a minimum of $0.8 \times 10^{-3}\,°C^{-1}$ at $c = 0.50$, (50 at% Zn).

Reconsidering the Matthiessen's rule, for solid solutions of low solute concentrations, in terms of the relaxation times of the electrons, τ and τ_s of pure aluminium and the dissolved metal as [18]

$$\rho_{all} = \frac{m^*}{ne^2\tau_s} + \frac{m^*}{ne^2\tau} \quad (7)$$

where m^* is the effective mass of the free electron. Comparing Equations 3 and 7

$$\beta c(1 - c) = m^*/ne^2\tau_s \quad (8)$$

or

$$\beta c(1 - c) = \rho_T \tau/\tau_s \quad (9)$$

The total electron relaxation time of the electrons in the alloy can be given from the formula [18]

$$1/\tau_{all} = 1/\tau + 1/\tau_s \quad (10)$$

Substituting τ_s from Equation 10 into Equation 8 and using Equation 7

$$\beta c(1 - c) = \rho_T(\tau/\tau_{all} - 1) \quad (11)$$

or

$$\tau_{all}/\tau = 1/[1 + \beta c(1 - c)/\rho_T] \quad (12)$$

Comparing Equations 6 and 12

$$\alpha_{all}/\alpha = \tau_{all}/\tau \quad (13)$$

From Equations 12 and 13, we find that τ_{all} decreases with increasing concentration of dissolved metal in the alloy. The calculated values of τ_{all}/τ are listed in Table I together with α_{all}.

3.2. Electrical resistivity measurements

Specimens of pure aluminium, AZ1.3, AZ3.2 and AZ5.2 were chosen for resistivity measurements. After being homogenized for 30 min at 530 °C and subsequently quenched into water maintained at about 0 °C at a quenching rate of $\sim 1000\,°C\,s^{-1}$, the specimens were mounted within a few seconds. The resistivity was immediately measured as a function of temperature during continuous heating at a rate of $10\,°C\,min^{-1}$ from room temperature (RT) up to 500 °C. Fig. 3 shows the behaviour of $\Delta\rho$ as a function of temperature, where $\Delta\rho$ is the difference between the measured resistivity and that expected at the given temperature, i.e.

$$\Delta\rho = \rho_{T(meas)} - \rho_{T(exp)} \quad (14)$$

where $\rho_{T(exp)} \cong \rho_{RT}(1 + \alpha_{all}\Delta T)$, ρ_{RT} is the measured resistivity at RT, α_{all} is given in Table I for each zinc concentration and $\Delta T = T - RT$. According to the behaviour of $\Delta\rho$ with temperature rise, one can predict which process is taking place at the given temperature. A quick decrease in $\Delta\rho$ has been observed in the initial stage of temperature (RT–85 °C) which is believed to be attributed to the annihilation of the quenched-in defects (vacancies and small vacancy clusters). On raising the temperature above 85 °C, an increase in $\Delta\rho$ takes place reaching a maximum at about 150 °C, and then decreases again. The increase in $\Delta\rho$ in this range of temperature (85–150 °C) may be attributed to the initial decomposition of the supersaturated solid solutions via GP zone formation. Above 150 °C, the formed GP zones dissolve. The process of GP zone dissolution continues up to 200 °C.

In the temperature range 280–375 °C, a strong decrease in $\Delta\rho$ is observed. This behaviour can be interpreted as the solute zinc atoms precipitating in this temperature range. The observed minimum in $\Delta\rho$ at about 375 °C indicates that the precipitated material is maximum at this temperature. Above 375 °C, the dissolution of the precipitates starts, as indicated by the increase of $\Delta\rho$. The dissolution process of the precipitates continues up to about 430 °C. In the temperature range 280–360 °C, $\ln(\Delta\rho)$ is plotted against $(1/T)$ for AZ3.2 and AZ5.2 specimens, Fig. 4. An

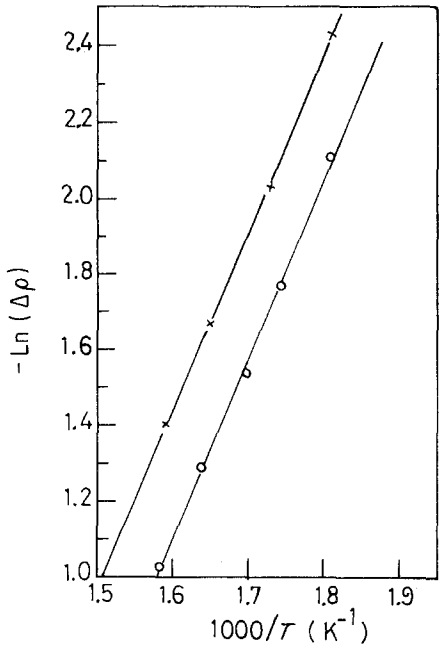

Figure 4 $\mathrm{Ln}(\Delta\rho)$ plotted against $1/T$ in the temperature range 280–360 °C for (×) AZ3.2 and (○) AZ5.2.

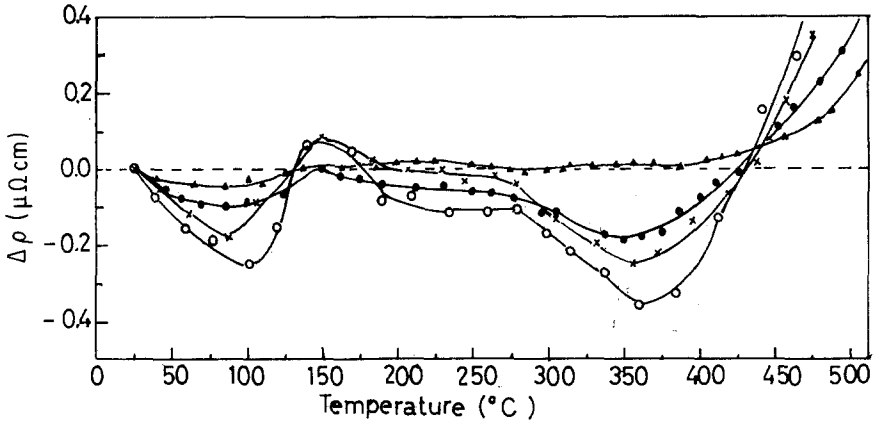

Figure 3 Behaviour of $\Delta\rho$ as a function of temperature during continuous heating for quenched (▲) pure aluminium, (●), AZ1.3, (×) AZ3.2 and (○) AZ5.2.

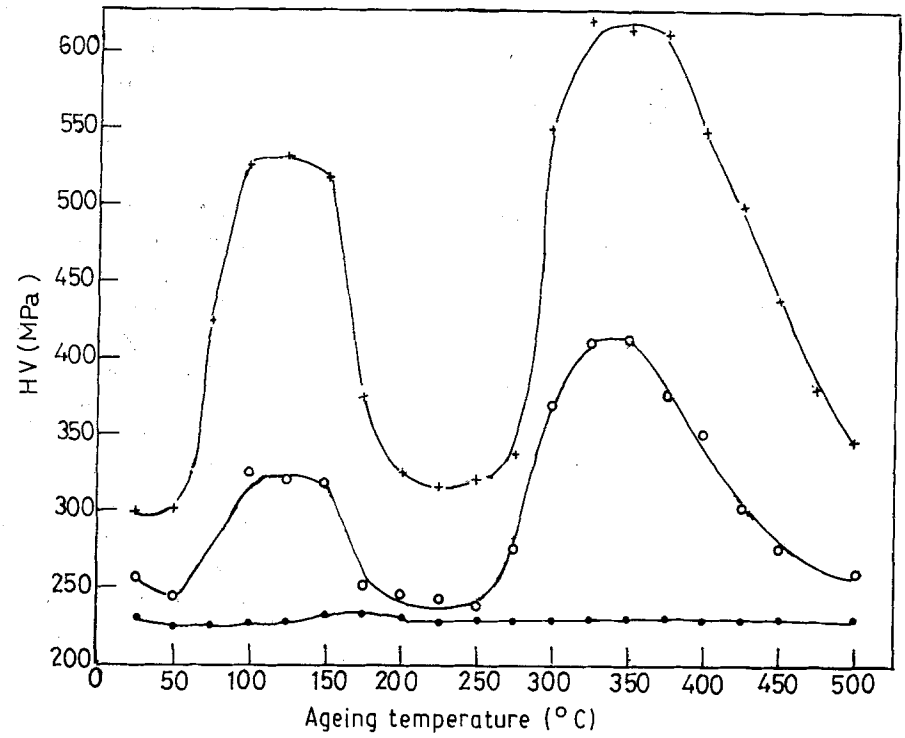

Figure 5 Behaviour of the microhardness, HV, of the quenched (●) pure aluminium, (○) AZ1.3 and (×) AZ3.2 as a function of ageing temperature.

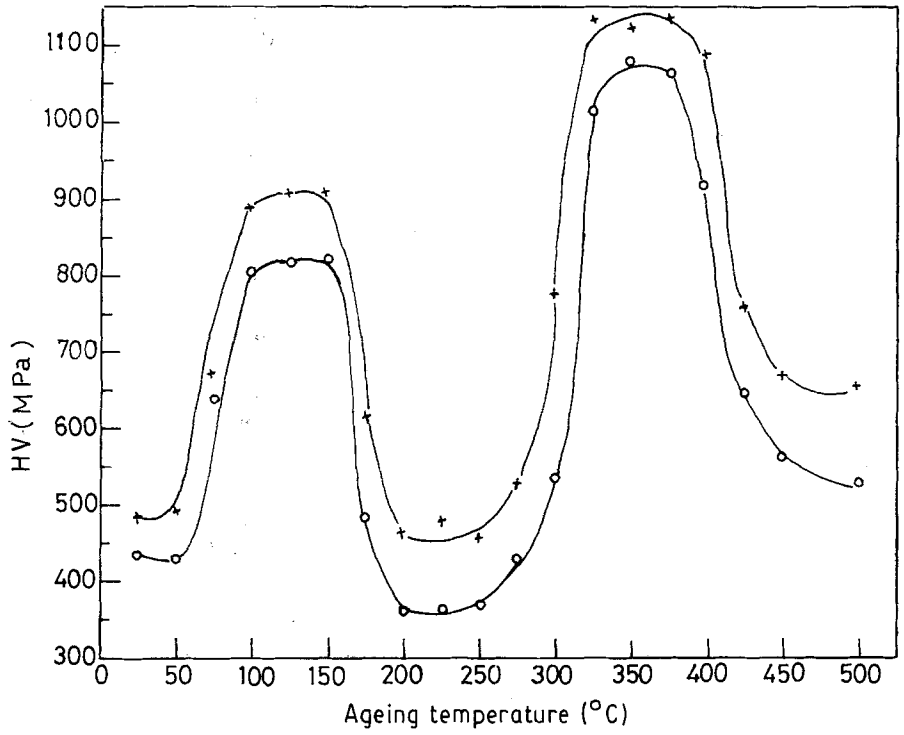

Figure 6 Behaviour of the microhardness, HV, of the quenched (○) AZ5.2 and (×) AZ6.4 specimens as a function of temperature.

activation energy of 0.41 eV has been obtained for the precipitation process, which is close to the migration energy of zinc atoms in aluminium [12]. On further heating, $\Delta\rho$ increases continuously, indicating that the generation of thermal vacancies predominates.

3.3. Microhardness measurements

Specimens of AZ1.3, AZ3.2, AZ5.2 and AZ6.4 were selected for the microhardness measurements. The same preceding solution heat treatment and quenching conditions were performed. In order to follow the variation of the microhardness of the specimens as a function of temperature, an isochronal ageing programme was performed. The specimens were aged for 10 min at 25 °C intervals from room temperature to 500 °C and then quenched into water maintained at 0 °C. The microhardness (HV) of the specimens was

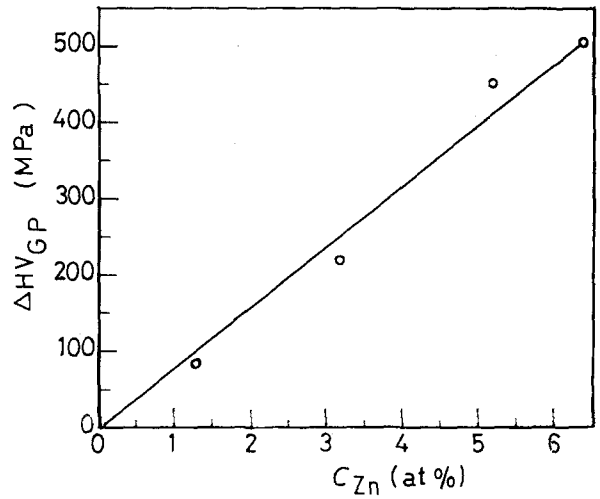

Figure 7 ΔHV_{GP} plotted as a function of zinc content, C_{Zn} at %.

measured at room temperature after each quench without paying attention to the impression positions. Each HV value is obtained from the average of at least ten readings distributed over the whole surface of the specimen.

Figs 5 and 6 show the variation of HV as a function of ageing temperature. It can be observed that all specimens have a similar behaviour. Figs 5 and 6 show a sharp increase in HV as the specimens were aged at a temperature higher than 50 °C. On ageing the specimens in the temperature range $100 \leqslant T \leqslant 150$ °C, HV has nearly constant values. This behaviour indicates that the GP zones have been completely formed by ageing the specimens at 100 °C. As the ageing temperature is raised above 150 °C, a sharp decrease in HV is measured. This rapid decrease is attributed to the dissolution of GP zones. The GP zone dissolution process continues up to ~ 200 °C. On ageing the specimens at temperatures higher than 275 °C, an increase in HV is observed, reaching a maximum at ~ 350 °C. This behaviour could be connected with the precipitation of zinc in aluminium, as the precipitation process is accompanied by a strong increase in HV. The observed decrease of HV above 375 °C, could be ascribed either to transition of the precipitates into noncoherent precipitates or to their dissolution.

To determine the contribution of GP zones to the microhardness of the alloys, ΔHV_{GP} (the difference between the measured microhardness of the given specimen containing the GP zones and that measured after the complete dissolution of the zones) is represented as a function of the zinc concentration, C_{Zn} at%, Fig. 7. The slope of the straight line obtained indicates that the formation of GP zones causes an increase in the microhardness of the alloy by an amount of about 80 MPa/at% Zn.

4. Discussion

It has been shown from Equations 6 and 12 that both the temperature coefficient of resistivity of the alloys, α_{all}, and the relaxation time of the free electrons in the alloys, τ_{all}, diminish with the concentration of the dissolved zinc, Table I. Namely, $1/\alpha_{all}$ varies linearly with $c(1 - c)$. In contrast, it has been reported that the temperature coefficient of resistivity, α_{all}, is nearly constant up to ~ 49.3 at% Zn [20]. This information seems to be unreasonable because α_{all} depends on the concentration of zinc as shown in Equation 6. However, in Al–Mg alloys, the temperature coefficient of resistivity was found experimentally to decrease exponentially with magnesium concentration up to ~ 27 at% Mg [20]. On the other hand, the decreasing behaviour of the relaxation times of free electrons, τ_{all}, with increasing concentration of zinc, agrees with the results of Logunov and Zverev [18] for Al–Mg alloys. This behaviour seems to be acceptable as the relaxation times are directly dependent on the mobility of the carriers. Because the carrier mobility decreases with increasing the scattering centres (impurities), the relaxation times should decrease as the concentration of impurities (zinc) increases.

The early stage decomposition and formation of fine-scale spherical GP zones in Al–Zn alloys which are coherent with the base lattice, results in a large contribution to the microhardness (80 MPa/at% Zn). In addition, the appearance of small-scale clusters (GP zones) is able to increase the electrical resistivity level with respect to the quenched state [11]. This phenomenon was explained in terms of the scattering power of the solute atom clusters which can be reinforced by a diffraction effect.The consistency of the resistivity increase with microhardness in the temperature range 85–150 °C confirmed that this phenomenon is connected with the formation of GP zones. The highest temperature at which the formation of GP zones is completed, is defined as the temperature limit for GP zone formation, T_{limit}. It was demonstrated that T_{limit} is the only way to explain the metastable miscibility gaps in the alloy systems [21]. Furthermore, for binary systems, it has been shown that T_{limit} and the solvus temperature of GP zones are in good agreement [21]. According to these statements, T_{limit} = 150 °C can be considered as the solvus temperature of the GP zones. Our results are in agreement with those obtained by Ohta *et al.* [14] from ageing and reversion studies of Al + 4.6 and Al + 5.6 at% Zn by means of microhardness measurements. However, they found that the reversion temperature of GP zones depends on the quenching temperature and ageing temperatures before the isochronal annealing programme has been started. The discrepancy between the obtained reversion temperatures was attributed to the heterogeneity of the vacancy concentrations which depend on the quenching temperature.

In the temperature range 275–350 °C, both the decrease in the resistivity, Fig. 3, and the increase in HV, Figs. 5 and 6, should be related to the process of the precipitation of the solute atoms. The increase in HV in this range of temperature indicates that the precipitates are coherent with the base lattice. This interpretation is based on the fact that the coherent precipitates cause a strong increase in the microhardness, while incoherent precipitates make a limited contribution to the microhardness of the alloys. The obtained value of the activation energy for the precipitation

TABLE II

	Formation of GP zones	Full-zoned alloy	Diss. GP zones	Zinc precip.	Diss. of precipitates
T°(C)	50–100	100–150	150–200	250–300	375–450

process of 0.41 eV is approximately equal to the migration energy of zinc atoms in aluminium [12]. Thus, the precipitation mechanism could be characterized by the migration and coalescence of zinc atoms to a microscopically large-scale zinc-rich clusters.

The decrease in HV above 375 °C could be ascribed either to the loss of coherency of the precipitates or to their dissolution. In this case, the differentiation between the two processes is not available because both the techniques used are indirect ones. Owing to the consistency of the resistivity increase and the HV decrease that have occurred above 375 °C, Figs 4–6, one can predict that the process is the dissolution of the zinc precipitates. Therefore from the preceding results one can tabulate the characteristic temperatures of the formation of GP zones, the dissolution of GP zones, precipitation of solute atoms and the dissolution of the precipitates in Table II.

Comparing the results of resistivity, Fig. 4, and those of HV measurements, Figs 5 and 6, one can notice that the characteristic temperatures of the corresponding processes are slightly higher in the case of Fig. 4. This discrepancy is believed to be due to the lack of equilibrium, because the measurements were done during the continuous heating of the specimens.

5. Conclusions

1. The electrical resistivity increase due to alloying is found to be proportional to the product of atomic fractional constituents (zinc and aluminium) and can be given as $\Delta\rho_{all} = 46.667 \times 10^{-6}\, c(1-c)\Omega\,\text{cm}$.

2. The temperature coefficient of resistivity, α_{all}, decreases with increasing concentration of the dissolved zinc in the alloy according to the relation $\alpha_{all} = \alpha/[1 + \beta c(1-c)/\rho_T]$.

3. The ratio of the temperature coefficient of resistivity of the alloy to that of pure aluminium, α_{all}/α, is equal to the ratio of the relaxation time of the free electrons in the alloy to that of pure aluminium, τ_{all}/τ, i.e. in dilute Al–Zn alloys, $\alpha_{all}/\alpha = \tau_{all}/\tau$.

4. The formation of GP zones takes place in the temperature range 50–100 °C, and results in an increase in the microhardness of the alloy by an amount of 80 MPa/at% Zn.

5. An activation energy of 0.41 eV is obtained for the precipitation process which is close to the migration energy of zinc atoms in aluminium indicating that the mechanism of the precipitation is characterized by the migration and coalescence of zinc atoms.

References

1. M. SIMERSKÁ and V. SYNEČEK, *Acta. Metall.* **15** (1967) 223.
2. J. ALLAIN and A. NAUDON, *Scripta Metall.* **8** (1974) 831.
3. K. B. RUNDMAN and J. E. HILLIARD, *Acta Metall.* **15** (1967) 1025.
4. G. WENDROCK, *Phys. Status Solidi (a)* **78** (1983) 497.
5. M. RADOMSKY, O. KABISCH, H. LÖFFLER, J. LENDVAI, T. UNGÁR, I. KOVÁCS and G. HONYEK, *J. Mater. Sci.* **14** (1979) 2906.
6. G. HONYEK, I. KOVÁCS, J. LENDVAI, NG-HUYSINH, T. UNGÁR, H. LÖFFLER and R. GERLACH, *ibid.* **16** (1981) 2701.
7. R. RAMLAU and H. LÖFFLER, *Phys. Status Solidi (a)* **79** (1983) 141.
8. V. L. SENDOV, V. A. TEIMURAZOVA and K. BARNDT, *Phys. Lett. A* **33** (1970) 319.
9. A. GABER, N. AFIFY and M. S. MOSTAFA, *J. Phys. D Appl. Phys.* **23** (1990) 1119.
10. A. GABER, *J. Mater. Sci. Mater. Electron.* **1** (1990) 137.
11. N. LUIGGI, J. P. SIMON and P. GUYOT, *Acta Metall.* **28** (1980) 1115.
12. A. JUHÁSZ, I. KOVÁCS, J. LENDVAI and P. TASNÁDI, *J. Mater. Sci.* **20** (1985) 624.
13. A. JUHÁSZ, P. TASNÁDI, I. KOVÁCS and T. UNGÁR, *ibid.* **16** (1981) 367.
14. M. OHTA, T. KANADANI, A. SAKAKIBARA, H. YAMADA and M. YAMADA, *Phys. Status Solidi(a)* **77** (1983) K49.
15. *Idem, ibid.* **78** (1983) K23.
16. M. OHTA, M. YAMADA, T. KANADANI and A. SAKAKIBARA, *Trans. Jpn Inst. Metals* **28** (1987) 615.
17. G. I. EPIFANOV, "Solid State Physics" (Mir Moscow, 1979).
18. A. V. LOGUNOV and A. F. ZVEREV, *Inzhenerno-Fisicheskii Z.* **15** (1969) 1114.
19. R. C. WEAST (ed.) "Handbook of Chemistry and Physics" (CRC, Cleveland, OH, 1978-9).
20. L. F. MONDOLFO, "Aluminium Alloys, Structure and Properties" (Butterworths, London, 1967).
21. H. INOUE, T. SATO, Y. KOJIMA and T. TAKAHASHI, *Metall. Trans.* **12A** (1981) 1429.

Received 7 January
and accepted 13 May 1991